
Revisiting Recurrent Reinforcement Learning with Memory Monoids

Steven Morad¹ Chris Lu² Ryan Kortvelesy¹ Stephan Liwicki³ Jakob Foerster² Amanda Prorok¹

Abstract

Memory models such as Recurrent Neural Networks (RNNs) and Transformers address Partially Observable Markov Decision Processes (POMDPs) by mapping trajectories to latent Markov states. Neither model scales particularly well to long sequences, especially compared to an emerging class of memory models sometimes called linear recurrent models. We discover that we can model the recurrent update of these models using a *monoid*, leading us to reformulate existing models using a novel *memory monoid* framework. We revisit the traditional approach to batching in recurrent RL, highlighting both theoretical and empirical deficiencies. We leverage the properties of memory monoids to propose a batching method that improves sample efficiency, increases the return, and simplifies the implementation of recurrent loss functions in RL.

1. Introduction

Reinforcement learning (RL) focuses on solving Markov Decision Processes (MDPs), although in many interesting problems we cannot access the Markov state directly. Outside of simulators, we instead receive noisy or ambiguous *observations*, resulting in Partially Observable MDPs. The standard approach to RL under partial observability is to summarize a sequence of observations into a latent Markov state using a *memory model* (sometimes called a sequence model). Often, these memory models are either RNNs or Transformers.

Unfortunately, it is expensive to train Transformers or RNNs over long sequences. Instead, prior work often truncates then zero-pads observation sequences into fixed length *segments*, keeping the maximum sequence length short. Using segments adds implementation complexity,

¹Department of Computer Science and Technology, University of Cambridge ²Department of Engineering Science, University of Oxford ³Toshiba Europe Ltd.. Correspondence to: Steven Morad <sm2558@cam.ac.uk>.

Code available at <https://github.com/proroklab/memory-monoids>. Copyright 2024 by the author(s).

reduces efficiency, and introduces theoretical issues. That said, most prior work and virtually all existing RL libraries follow this segment-based approach.

A new class of sequence models, sometimes called Linear Recurrent Models or Linear Transformers, is much more efficient over long sequences. These models can be parallelized over the sequence dimension while retaining sub-quadratic space complexity. We find that many such models can be rewritten as a *memory monoid*, a unifying framework for efficient memory models that we define in this paper. Since these efficient models do not share sequence length limitations with past models, we question *whether the use of segments is still necessary*.

Contributions In this work, we propose a unifying framework for efficient memory modeling, then propose an alternative batching method reliant on our framework. Our method improves sample efficiency across various tasks and memory models, while generally simplifying implementation.

1. We propose the *memory monoid*, a unifying framework for efficient sequence models. In particular, we
 - Reformulate existing sequence models as memory monoids
 - Derive memory monoids for the discounted return and advantage, leveraging GPU parallelism
 - Discover a method for inline resets, enabling any memory monoid to span multiple episodes
2. We investigate the impact that segments have on reinforcement learning. Specifically, we
 - Highlight theoretical shortcomings of sequence truncation and padding, then demonstrate their empirical impact
 - Propose a batching method that improves sample efficiency across all tested models and tasks, while also simplifying recurrent loss functions

2. Preliminaries and Background

Consider an MDP $(S, A, R, \mathcal{T}, \gamma)$, where at each timestep t , an agent produces a transition $T = (s, a, r, s')$ from interaction with the environment. We let $s, s' \in S$ denote

the current and next states and state space, $a \in A$ denote the action and action space, $R : S \times A \times S \mapsto \mathbb{R}$ denote the reward function, and $\mathcal{T} : S \times A \mapsto \Delta S$ denote the state transition matrix (Δ denotes a distribution). In RL, our goal is to learn a stochastic policy parameterized by θ that maps states to action distributions $\pi_\theta : S \mapsto \Delta A$. The agent samples an action from the policy given the current state $a \sim \pi_\theta(s)$, and stochastically transitions to the next state $s' \sim \mathcal{T}(s, a)$, receiving a reward $r = R(s, a, s')$. The optimization objective is to find the parameters θ that maximize the expected return, discounted by γ : $\mathbb{E}[\sum_{t=0}^{\infty} \gamma^t R(s_t, a_t, s_{t+1}) \mid \mathcal{T}(s_{t+1}|s_t, a_t), \pi(a_t|s_t)]$.

2.1. Rollouts, Causality, and Episode Boundaries

It is often practical to model terminal states in MDPs, such as a game over screen in a video game. In a terminal state, all actions lead back to the terminal state and the discounted return after entering the terminal state is always zero. We mark whether a state is terminal using the *done flag* $d \in \{0, 1\}$. The done flag is stored in the transition $T = (s, a, r, s', d)$.

When considering RL loss functions, it is conceptually helpful to think in terms of transition tuples. However, while navigating the MDP we do not have access to the full transition. We receive just the state at the current timestep – the MDP emits the reward and done flag corresponding to the current state, as well as the next state (r, d, s') during the following timestep.

We find that our paper is more clear if we introduce a *begin flag* $b \in \{0, 1\}$ that is emitted alongside each observation, available during both training and inference. The begin flag is 1 at the initial timestep of an episode and 0 otherwise. We differentiate between a transition $T = (s, a, r, s', b, d)$ available only in hindsight, and a partial transition $\bar{T} = (s, b)$ as emitted while navigating the MDP. The partial transition enables us to remove any ambiguities with respect to episode boundaries during training, inference, or within memory models.

At each policy update, we interact with the environment to produce a *rollout* of transitions $\rho = (T_1, T_2, \dots, T_n)$. We may either train the policy on these transitions immediately, or store them in a replay buffer for later use.

2.2. Partial Observability

In partially observable settings, we cannot directly measure the Markov state s . Instead, we indirectly measure s via the observation $o \sim \mathcal{O}(s)$, following the observation function $\mathcal{O} : S \rightarrow \Delta O$. With the observation replacing the state, interaction with the environment now produces a transition $T = (o, a, r, o', d, b)$ and partial transition $\bar{T} = (o, b)$. For certain tasks, the action from the previous timestep is also

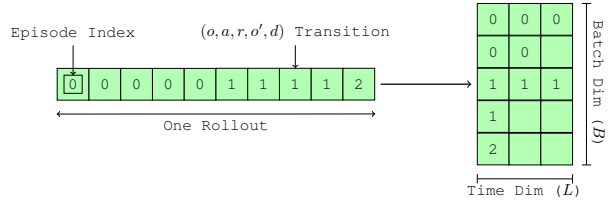


Figure 1. We visualize the Segment-Based Batching approach often used in prior literature. A worker collects episodes, which are split and zero-padded to produce a batch of segments, each with a constant, user-specified segment length L . Episodes exceeding the specified length are broken into multiple segments, preventing backpropagation through time from reaching earlier segments. This approach reduces efficiency, biases normalization methods, and requires specialized recurrent loss functions.

necessary, and is implicitly included in the observation.

A sequence of transitions starting where $b = 1$ and continuing until a terminal state is known as an episode E . We use a memory model M to summarize the corresponding sequence of partial transitions into a latent Markov state.

$$M : \bar{T}^n \mapsto S^n. \quad (1)$$

If M is recurrent, we may alternatively write M as

$$M : H \times \bar{T} \mapsto H \times S, \quad (2)$$

where H is the set of recurrent states.

Memory models process all partial transitions in the order which they occurred. Each episode E often contains a variable number of transitions, making it difficult to store, batch, or efficiently train over more than one episode at a time.

2.3. Segment-Based Batching

In RL, we often wish to reason over batches of data. Under partial observability, a batch would consist of multiple sequences (episodes). Recall that episodes can vary in length, so how is one to effectively batch over variable-length episodes? The solution used in prior literature and virtually all RL libraries is the use of *segments* (Hausknecht & Stone, 2015; Kapturowski et al., 2019; Hafner et al., 2023; Bauer et al., 2023; Liang et al., 2018; Raffin et al., 2021; Huang et al., 2021; Serrano-Muñoz et al., 2023).

In *Segment-Based Batching* (SBB), we split and zero pad episodes so that they can be stacked into a tensor with batch and sequence length dimensions $B \times L$. Each row in this tensor is a segment σ containing exactly L transitions.

Episodes longer than L transitions will be split into multiple *fragments*, such that each is at most L transitions. Fragments shorter than L transitions will be zero padded

from the right, such that they become exactly length L . We call these length L fragments *segments*. We must also store a mask m denoting which elements are zero-padding and which are data. The segments and masks are stacked along the batch dimension, creating $B \times L$ matrices for storage and training (Figure 1). We formally define SBB in Appendix C.

The Shortcomings of Segments SBB introduces a number of shortcomings. The zero padding and associated masks must be stored, taking up additional space. The zero padding is fed to the memory model, wasting computation on zeros that are discarded during gradient computation. The zero padding also prevents the use of BatchNorm (Ioffe & Szegedy, 2015) and other normalization methods by shifting the mean and variance of input data. The extra time dimension and padding complicates RL loss functions. Most importantly, when SBB splits episodes into distinct segments, it changes the loss gradient.

Let us inspect the effect of SBB on the memory model gradient. Assume we have a loss function \mathcal{L} defined over a memory model parameterized by θ . The true gradient of the loss over an episode of length n is

$$\nabla = \frac{\partial \mathcal{L}(\theta, (T_0, T_1, \dots, T_{n-1}))}{\partial \theta}. \quad (3)$$

In SBB, we split episodes into length L segments. We approximate the gradient over these segments as

$$\nabla_{\sigma} = \sum_{j=0}^{n/L} \frac{\partial \mathcal{L}(\theta, (T_{jL}, \dots, T_{2j(L-1)}))}{\partial \theta}. \quad (4)$$

Under SBB, we compute the gradient independently for each segment. The gradient across segment boundaries (addends) is therefore always zero. With zero gradient across boundaries, it is unlikely that temporal dependencies greater than the segment length L can be learned. Prior work (Hausknecht & Stone, 2015; Kapturowski et al., 2019) assumes that $\nabla \approx \nabla_{\sigma}$, although we are not aware of any theoretical justification for this assumption, as the error between the true and approximated gradient is unbounded.

2.4. On the Efficiency of Sequence Models

SBB evolved alongside RNNs in RL (Hausknecht & Stone, 2015), and Transformers to a lesser extent. By setting the sequence length L to be small, SBB makes RNNs and Transformers tractable.

Both Transformers and RNNs struggle over long sequences. RNNs rely on the previous recurrent state to compute the following recurrent state, prohibiting parallelism over the time dimension. Thus, they are unable to exploit the parallelism of modern GPUs over the time dimension.

Transformers use pairwise attention on the sequence elements, scaling quadratically in space on the length of the sequence.

A recent class of models espouse time-parallel execution while being either linear or subquadratic in space complexity. These models, such as State Space Models, Linear Transformers, Fast Weight Programmers, RetNet, RWKV, Linear Recurrent Units, and Fast and Forgetful Memory (Gu et al., 2021; Katharopoulos et al., 2020; Schlag et al., 2021; Anonymous, 2023; Peng et al., 2023; Orvieto et al., 2023; Morad et al., 2023b) are sometimes called *Linear Recurrent Models* because they either have quasi-linear space complexity, or alternatively employ a linear recurrent state update (e.g., $\dot{x} = Cx + c$).

3. A Functional Approach to Recurrent Models

As stated in the previous section, many Linear Recurrent Models utilize a linear recurrent state update. This linear update is one example of a *monoid* (Bourbaki, 1965) – a concept from category theory with use in functional programming.

Definition 3.1. A tuple (H, \bullet, H_I) is a monoid if:

The binary operator \bullet is closed on H (5)

$$(a \bullet b) = c, \quad a, b, c \in H$$

The binary operator \bullet is associative (6)

$$(a \bullet b) \bullet c = a \bullet (b \bullet c), \quad a, b, c \in H$$

There exists an identity element H_I (7)

$$(H_I \bullet a) = (a \bullet H_I) = a \quad a, H_I \in H,$$

where \bullet for a single input a is defined as $(\bullet a) = (H_I \bullet a)$.

Unlike prior Linear Time Invariant (LTI) models (e.g., State Space Models), the binary operator \bullet *need not be linear or time invariant*. For example, $\dot{x} = \text{ReLU}(Cx + c)$ is nonlinear and Fast and Forgetful Memory is time-varying (Appendix G), (Morad et al., 2023a).

Any monoid operator \bullet can be computed in parallel across the time dimension using a parallel scan (Dhulipala et al., 2021). Given a sequence of length n , a work-efficient parallel scan known as the Blelloch Scan executes $O(n)$ calls to \bullet in $O(n)$ space to produce n outputs (Blelloch, 1990). With p parallel processors, the parallel time complexity of the scan is $O(n/p + \log p)$. For large GPUs where $n = p$, the parallel time complexity becomes $O(\log n)$.

While powerful, standard monoids are defined only over the recurrent state space H . In memory models we often decouple the Markov state space S from the recurrent state space H (Equation 2), as in many cases a low dimensional

Markov state could be represented as a function of a higher dimensional recurrent state. In search of more general sequence models, we extend the monoid with the *memory monoid*.

Definition 3.2. $((H, \bullet, H_I), f, g)$ constitute a memory monoid if (H, \bullet, H_I) defines a monoid and functions f, g are:

An encoder, mapping from a partial transition to the right argument of \bullet (8)

$$f : \bar{T} \mapsto H$$

A decoder, mapping an updated recurrent state and a partial transition to a Markov state (9)

$$g : H \times \bar{T} \mapsto S$$

Recall that a partial transition consists of the observation and begin flag $\bar{T} = (o, b)$. We define a recurrent memory model $M : H \times \bar{T} \mapsto H \times S$ (Equation 2) using our memory monoid, where M is the sequence of two operations:

(1) Update the recurrent state (10)

$$A' = A \bullet f(\bar{T}), \quad A, A' \in H$$

(2) Produce an output from the updated recurrent state

$$s = g(A', \bar{T}), \quad A' \in H, s \in S. \quad (11)$$

Thus, we can execute any memory monoid as

$$h_t = h_{t-1} \bullet f(\bar{T}), \quad h_t, h_{t-1} \in H \quad (12)$$

$$s_t = g(h_t, \bar{T}) \quad (13)$$

Given n inputs, functions f and g can each be split into n concurrent threads, as f, g have no dependencies on previous sequence elements. Consequently, *all memory monoids have logarithmic parallel time complexity and linear space complexity on the length of the sequence*⁴.

3.1. Reformulating Existing Sequence Models

As an exercise in the flexibility of our memory monoid, let us reformulate an existing memory model as a memory monoid. The Linear Transformer from (Katharopoulos et al., 2020) can be reformulated as

$$H = \{(A, a) \mid A \in \mathbb{R}^{j \times k}, a \in \mathbb{R}^j\} \quad (14)$$

$$H_I = (0, 0) \quad (15)$$

$$(A, a) \bullet (A', a') = (A + A', a + a') \quad (16)$$

$$f(o, b) = ((W_k o)(W_v o)^\top, W_k o) \quad (17)$$

$$g((A, a), (o, b)) = \text{MLP} \left(\frac{AW_q o}{a^\top W_q o} \right). \quad (18)$$

⁴Assuming (1) The binary operator \bullet is constant-time and constant-space, which is the case for all models listed thus far. (2) Our processor has n parallel threads of execution, where n is the length of the sequence.

We scan the Linear Transformer memory monoid over a sequence of partial transitions following (Definition 3.2) to produce recurrent and Markov states

$$[h_0 \ h_1 \ \dots] = [H_I \bullet f(\bar{T}_0) \ H_I \bullet f(\bar{T}_0) \bullet f(\bar{T}_1) \ \dots] \quad (19)$$

$$[s_0 \ s_1 \ \dots] = [g(\bar{T}_0, h_0) \ g(\bar{T}_1, h_1) \ \dots] \quad (20)$$

where $h_j = (A_j, a_j)$.

We rewrite the S5 variant of State Space Models, the Linear Recurrent Unit, and Fast and Forgetful Memory (Lu et al., 2024; Orvieto et al., 2023; Morad et al., 2023b) as memory monoids in Appendix G.

3.2. Accelerated Discounted Returns

We find that memory monoids can model other recurrences as well. For example, we can rewrite the discounted return as a memory monoid, computing it in a *GPU-efficient* fashion using a high-level framework like JAX (Bradbury et al., 2018)

Theorem 3.3. *The discounted cumulative return given by*

$$G = \sum_{t=0}^{\infty} \gamma^t r_t \quad (21)$$

is equivalent to computing M (Definition 3.2) over r_0, r_1, \dots for the following memory monoid:

$$H = \{(a, r) \mid a \in [0, 1], r \in \mathbb{R}\} \quad (22)$$

$$H_I = (1, 0) \quad (23)$$

$$(a, r) \bullet (a', r') = (aa', ar' + r) \quad (24)$$

$$f(o, b) = (\gamma, o) \quad (25)$$

$$g((a, r), (o, b)) = r. \quad (26)$$

Proof. See Appendix D. \square

Our experiments show that executing the return memory monoid on the GPU provides a significant speed up. In Appendix F, we prove that Generalized Advantage Estimation (GAE) (Schulman et al., 2016) targets can also be rewritten as a memory monoid.

3.3. Inline Recurrent State Resets

So far, we have assumed that we operate over a single episode using the Belloch Scan. Consider that in RL, we traditionally operate over multiple episodes at once, often each with differing lengths. To scan over a batch, we could truncate and zero pad sequences such that each is a fixed length (i.e., SBB), however this introduces issues explained in Section 2.3. Furthermore, this approach would not work with quantities such as the return.

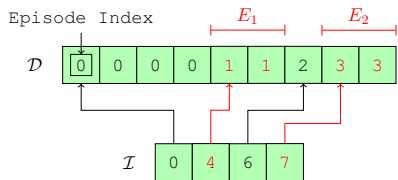


Figure 2. A visualization of sampling in TBB, with a batch size of $B = 4$. Transitions from rollouts are stored in-order in \mathcal{D} , while associated episode begin indices are stored in \mathcal{I} . We sample a train batch by randomly selecting from \mathcal{I} . For example, we might sample 4 from \mathcal{I} , corresponding to E_1 in red. Next, we sample 7 from \mathcal{I} , corresponding to E_2 in red. We concatenate $\mathcal{B} = \text{concat}(E_1, E_2)$ and return the result as a train batch.

Since memory monoids are efficient over long sequences, we could consider concatenating individual episodes into one very long sequence, removing the need for padding and truncation. Unfortunately, as the scan crosses episode boundaries, it feeds information from all prior episodes into future episodes, and information from future episodes into preceding episodes.

To resolve this issue, we propose a *resettable monoid transformation*, which prevents information from leaking across episode boundaries. We can apply this transformation to any monoid (or memory monoid), to produce a new monoid that respects episode boundaries.

Theorem 3.4. *All monoids (H, \bullet, H_I) can be transformed into a resettable monoid (G, \circ, G_I) defined as*

$$G = \{(A, b) \mid A \in H, b \in \{0, 1\}\} \quad (27)$$

$$G_I = (H_I, 0) \quad (28)$$

$$(A, b) \circ (A', b') = ((A \cdot (1 - b') + H_I \cdot b') \bullet A', b \vee b') \quad (29)$$

For a single episode, the A term output by the operator \circ is equivalent to the output of \bullet . Over multiple contiguous episodes, \circ prevents information flow across episode boundaries.

Proof. See Appendix D. \square

By transforming the monoid (H, \bullet, H_I) within a memory monoid, we no longer require separate time and batch dimensions during training. Now, we can process a long sequence as if it were many distinct episodes.

4. Tape-Based Reinforcement Learning

Training over the concatenation of episodes would be intractable using Transformers or RNNs due to poor sequence length scaling, while Linear Recurrent Models leak information between episodes. By combining the efficiency of memory monoids with our resettable transform,

we resolve these issues, enabling us to fold the batch and time dimensions into a single dimension. We call this approach *Tape-Based Batching* (TBB), which consists of two operations: *insertion* and *sampling*.

4.1. Insertion

As we collect transitions for training, we often want to store them for later. We store them following Algorithm 1.

Algorithm 1 Inserting transitions using TBB

Input: List of transitions \mathcal{D} , list of indices \mathcal{I} , buffer size D
Output: List of transitions \mathcal{D} , list of indices \mathcal{I}
 $\rho \leftarrow (T_0, T_1, \dots, T_{n-1})$ {Collect rollout from env}
if on-policy **then**
 $\mathcal{D} \leftarrow \rho$
 $\mathcal{I} \leftarrow \text{where}(b_0, \dots, b_{n-1})$ {Indices of new episodes}
else
 while $(\mathcal{D} + \text{card}(\rho)) > D$ **do**
 $\mathcal{I} \leftarrow \mathcal{I}[1 :]$ {Buffer full, pop oldest index}
 $\mathcal{D} \leftarrow \mathcal{D}[\mathcal{I}[0] :]$ {Pop transitions for the oldest episode}
 end while
 $\mathcal{I} \leftarrow \text{concat}(\mathcal{I}, \text{card}(\mathcal{D}) + \text{where}(b_0, \dots, b_{n-1}))$ {Idx}
 $\mathcal{D} \leftarrow \text{concat}(\mathcal{D}, \rho)$ {Update buffer}
end if

We maintain ordered lists of transitions \mathcal{D} , and begin indices \mathcal{I} , corresponding to episode boundaries in \mathcal{D} . We update \mathcal{I} based on the begin flags in the rollout, then append the rollout transitions to our dataset \mathcal{D} .

Upon reaching the maximum capacity of \mathcal{D} , we must discard old transitions to make room for new ones. To make room, we pop the episode begin index from the left of \mathcal{I} and discard the resulting episode in \mathcal{D} . Popping \mathcal{I} from the left discards the oldest episode. We repeat this process until \mathcal{D} can fit the new episodes.

This method works both for rollouts that contain complete episodes ($d_{n-1} = 1$), and those that contain incomplete episodes ($d_{n-1} \neq 1$), where a rollout might stop before finishing an episode. When combining incomplete episodes with multiple rollout workers, we can experience race conditions. In this scenario, it is easiest to keep one \mathcal{D}, \mathcal{I} per worker to prevent race conditions.

4.2. Sampling

Once we have constructed \mathcal{D}, \mathcal{I} , we are ready to train a policy or compute returns. We sample transitions from the buffer following Algorithm 2.

If we are training on-policy, we can simply train on \mathcal{D} . If we are training off-policy, we randomly sample a training batch \mathcal{B} from our dataset. First, we randomly sample an index without replacement. We slice \mathcal{D} using the sampled and next indices to retrieve a random full episode. We continue this process, concatenating our slices together

Algorithm 2 Sampling transitions using TBB

Input: List of transitions \mathcal{D} , list of indices \mathcal{I} , batch size B
Output: Batch of transitions \mathcal{B}
 $\mathcal{B} \leftarrow ()$ {Empty list}
while $\text{len}(\mathcal{B}) < B$ **do**
 $i \sim \mathcal{U}(0, \text{card}(\mathcal{I}) - 1)$ {Randomly sample an index in \mathcal{I} }
 $\mathcal{B} \leftarrow \text{concat}(\mathcal{B}, D[\mathcal{I}[i] : \mathcal{I}[i + 1]])$ {Append ep. to batch}
end while
 $\mathcal{B} = \mathcal{B}[: B]$ {Make batch exactly B transitions}

until they reach the user-defined batch size B , truncating the final episode if necessary (Figure 2). One could extend our sampling approach to implement Prioritized Experience Replay (Schaul et al., 2015) by assigning each episode/index in \mathcal{I} a priority.

4.3. Simplifying the Loss Functions

With TBB, we utilize unmodified, non-recurrent loss functions to train recurrent policies, reducing the implementation complexity of recurrent RL algorithms. Unlike SBB, there is no need to mask outputs or handle additional time dimensions like in SBB. With TBB, the only difference between a recurrent and nonrecurrent update is precomputing the Markov states s, s' before calling the loss function. We demonstrate this by writing the TBB Q learning update in Algorithm 3, highlighting departures from the standard, non-recurrent Q learning update in red.

For posterity, we define the standard SBB Q learning update in Algorithm 4. Note that the update equation has an additional time dimension k and requires a padding mask $m_{i,j}$.

Algorithm 3 TBB deep Q update

Input: params θ , target params ϕ , Q function Q , sequence model M , train batch \mathcal{B} , discount γ , target update rate β
Output: params θ, ϕ
 $(s_1, s_2, \dots, s_B) \leftarrow M_\theta(T_1, \dots, T_B)$ {Estimate Markov state}
 $(s'_1, s'_2, \dots, s'_B) \leftarrow M_\phi(T_1, \dots, T_B)$ {Next Markov state}
 $\hat{y}_j = r_j + \max_{a \in A} \gamma Q_\phi(s'_j, a)$, $\forall \mathcal{B}[j]$ {Compute target}
 $\theta \leftarrow \min_\theta \|Q_\theta(s_j, a_j) - \hat{y}_j\|$, $\forall \mathcal{B}[j]$ {Compute loss, update}
 $\phi \leftarrow \phi\beta + (1 - \beta)\theta$ {Update target params}

5. Experiments and Discussion

We begin our experiments with investigating the shortcomings of SBB, specifically the theoretical issues stemming from truncated backpropagation. We then compare TBB to SBB across a variety of tasks and models. Finally, we examine the wall-clock efficiency of memory monoids.

Our experiments utilize tasks from the POPGym benchmark (Morad et al., 2023a), and all TBB to SBB comparisons use identical hyperparameters and random seeds. We validate our findings across State Space Models (S5),

Algorithm 4 SBB deep Q update

Input: params θ , target params ϕ , Q function Q , sequence model M , train batch \mathcal{B} , discount γ , target update rate β
Output: params θ, ϕ
 $\begin{bmatrix} s_{1,1}, \dots, s_{1,L} \\ \vdots \\ s_{B,1}, \dots, s_{B,L} \end{bmatrix} \leftarrow \begin{bmatrix} M_\theta((T_{1,1}) \dots (T_{1,L})) \\ \vdots \\ M_\theta((T_{B,1}) \dots (T_{B,L})) \end{bmatrix}$
 $\begin{bmatrix} s'_{1,1}, \dots, s'_{1,L} \\ \vdots \\ s'_{B,1}, \dots, s'_{B,L} \end{bmatrix} \leftarrow \begin{bmatrix} M_\phi((T_{1,1}) \dots (T_{1,L})) \\ \vdots \\ M_\phi((T_{B,1}) \dots (T_{B,L})) \end{bmatrix}$
 $\hat{y}_{j,k} = (r_{j,k} + \max_{a \in A} \gamma Q_\phi(s'_{j,k}, a))$, $\forall \mathcal{B}[j, k]$
 $\theta \leftarrow \min_\theta m_{j,k} \cdot \|Q_\theta(s_{j,k}, a_{j,k}) - \hat{y}_{j,k}\|$, $\forall \mathcal{B}[j, k]$
 $\phi \leftarrow \phi\beta + (1 - \beta)\theta$

Linear Recurrent Units (LRU), Fast and Forgetful Memory (FFM), and the Linear Transformer (LinAttn) memory monoids. We train our policies using Double Dueling DQN (Van Hasselt et al., 2016; Wang et al., 2016). Our model architecture uses blocks consisting of linear layers, LayerNorm, and Leaky ReLU activation (Ba et al., 2016; Xu et al., 2015). Our model consists of one block, followed by the memory model, followed by two more blocks. See Appendix I for more detailed information.

What are the Consequences of Truncating BPTT? In Section 2.3, we discussed how the estimated (truncated) gradient used in SBB differs from the true gradient. Although there is no theoretical justification for why the estimated and true gradients should be similar, one could imagine that observations made outside the segment are from long ago and should have little impact on the Q value. We aim to determine whether the estimated gradient used in SBB is a sufficient approximation of the true gradient.

We approach this question by measuring the impact each observation has on the terminal Q value of an episode (i.e., $Q(s_n, a_n) = R(s_n, a_n, s_{n+1})$). We focus on the Repeat Previous task, where the agent must output an observation from ten timesteps ago. Any observations older than ten timesteps are not necessary and, given a relative-time policy, should have little to no impact on the terminal Q value. Recall that we can write a memory model as $s_n = M(o_0, \dots, o_n)$. We explicitly compute

$$\left| \frac{\partial Q(s_n, a_n)}{\partial o_i} \right| = \left| \frac{\partial Q(s_n, a_n)}{\partial s_n} \frac{\partial s_n}{\partial o_i} \right|, \quad (30)$$

and plot the results for FFM, S5, and LRU models in Figure 3. We also examine other model and task combinations in Appendix B.

Surprisingly, we see that virtually all previous observations significantly affect the Q value, across models and tasks. In other words, *learned recurrent Q functions do not generalize well over time*, although we find that policies trained with TBB generalize better.

In one case, roughly 90% of the Q value is produced outside the segment boundaries, where backpropagation cannot reach. One possible explanation for this long-tail gradient distribution is that the memory model is “counting” each observation to accurately predict when the episode terminates. Our findings suggest that SBB could be a major contributor to the increased difficulty and reduced sample efficiency of recurrent RL, as we demonstrate in the next experiment.

Is TBB More Sample Efficient? For our second experiment, we measure the difference in sample efficiency between TBB and SBB. There are two reasons that TBB could improve upon SBB sample efficiency: (1) As previously discovered, the truncated gradient used by SBB is often a poor estimate of the true gradient (2) SBB decreases the effective batch size through zero padding. We note that the cost of zero padding in SBB is equivalent to the cost of real data – it takes up equivalent space in the replay buffer and takes just as much compute to process as real data. We report some combinations of model and task in Figure 4 and present the full results in Appendix A.

We find that TBB produces a noticeable improvement in sample efficiency over SBB, across all configurations of memory model and environment. Even for large segments lengths $L = 100$, we find a significant gap between SBB and TBB. SBB must make an inherent tradeoff – it can use long segments to improve gradient estimates at the cost of smaller effective batch sizes, or shorter segments to improve the effective batch size at the expense of a worse gradient estimate. TBB does not need to make this tradeoff. In our experiments, SBB with larger L always outperforms shorter L , suggesting that the gradient estimation error is a larger contributor to SBB’s lackluster performance than reduced effective batch sizes.

Are Memory Monoids Fast in Practice? In Figure 5, we test the wall-clock efficiency of our discounted return monoid against the standard approach of iterating over episodes in a batch. Both the monoid and standard approach are just-in-time compiled on a GPU, however the standard approach requires a for loop when the episode lengths are not fixed. We sample a batch of episodes, where each episode length is sampled from a discrete uniform distribution between one and a maximum episode length. We find that our memory monoid computes the discounted return between three orders of magnitude faster.

Next, we compare TBB and SBB scaling. TBB scales worse than SBB ($O(\log B)$ and $O(\log L)$ respectively, where B is the batch size and L is segment length). We question how this overhead translates to wall-clock training time. In Table 1, we examine the total time spent training, finding that the time difference is negligible. The mem-

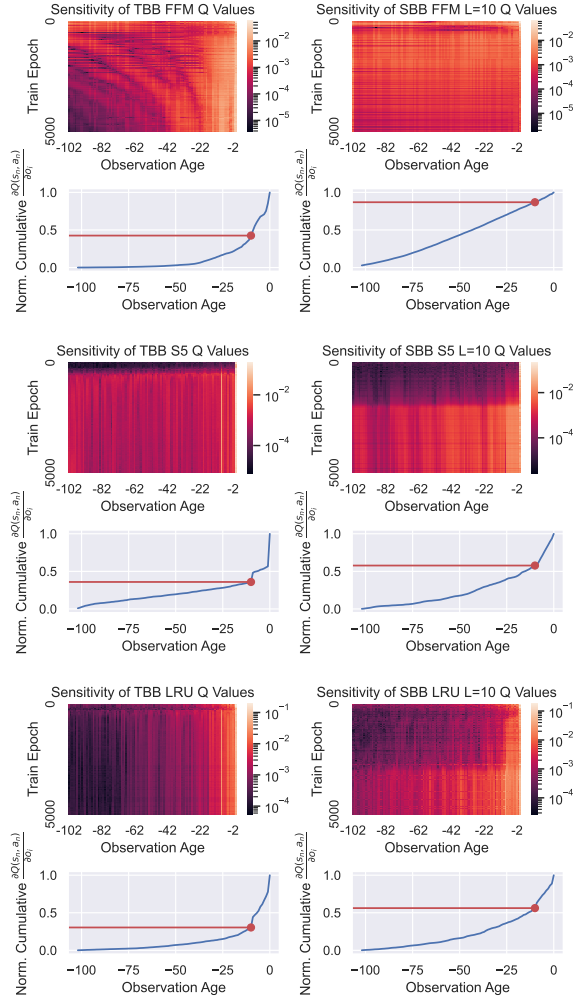


Figure 3. We demonstrate how SBB can hurt Q learning with FFM, S5, and LRU models, even with a segment length L sufficient to capture all necessary information. We train various models to convergence on the Repeat Previous task, where the agent must output the observation from 10 timesteps ago. To determine the impact each previous observation has on the Q value at the terminal transition, we compute the partial derivative with respect to the observations. This partial derivative determines how much each prior observation contributes to the Q value. We plot the results for each training epoch using a heatmap, and zoom in on the final training epoch using a CDF of the partials. In the CDF plots, the red line and dot correspond to 10 timesteps in the past, the point at which old observations should have no impact on the Q value. We see, however, that the observations older than 10 timesteps have a significant impact on Q values. For FFM trained with SBB $L = 10$, roughly 90% of the Q value is not learnable. There is no “safe” segment length L , in the sense that even the initial observation contributes a nonzero amount to the last Q value. This emphasizes how important our proposed TBB is, because it enables backpropagation over the entire sequence. We see that policies trained with TBB tend to be less sensitive to unnecessary inputs, suggesting that they generalize better.

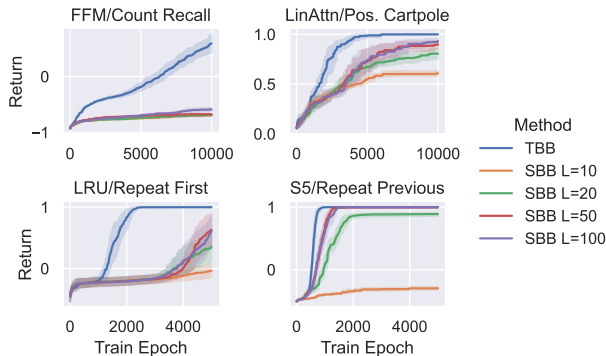


Figure 4. We compare TBB (ours) to SBB across POPGym tasks and memory models, reporting the mean and 95% bootstrapped confidence interval of the evaluation return over ten seeds. We find that TBB significantly improves sample efficiency.

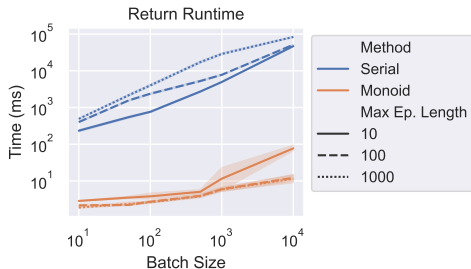


Figure 5. We compare how long it takes to compute the discounted return using our monoid, compared to the standard way of iterating through a batch. Computing the discounted return is orders of magnitude faster when using our monoid implementation. We evaluate ten random seeds on a RTX 2080Ti GPU.

ory model forward pass is only a fraction of the time spent at each epoch, with environment sampling, replay buffer sampling (and in the case of SBB, splitting, truncating, and padding sequences) all taking a nontrivial amount of time.

Limitations and Future Work According to our sensitivity analysis, old observations unexpectedly impacted the Q value across models and tasks. Perhaps linear updates are insufficient, and nonlinear update rules might generalize better across time.

In our experiments, we focused on long-term memory tasks from the POPGym benchmark, each of which tests a specific aspect of long-term memory. We did not experiment on environments like Atari, primarily because it is unclear to what extent Atari tasks require long-term memory.

Although memory monoids scale well to long sequences, TBB still pays an increased $\log B$ time cost compared with SBB’s $\log L$ cost. There was no perceptible difference in our experiments, but very long sequences such as those

Method	Train Time (s)	Std. Dev. (s)
SBB L=10	886.39	54.47
SBB L=20	886.30	49.71
SBB L=50	887.58	50.29
SBB L=100	886.25	49.87
TBB	886.87	53.21

Table 1. We report the time taken to train a policy from start to finish. We compare TBB against SBB with various segment lengths, on an RTX 2080Ti. We evaluate FFM, S5, LRU, and Linear Attention over ten seeds on the Repeat First task, reporting the mean over all, grouped by batching method. In practice, the performance differences between TBB and SBB seem insignificant.

used for in-context RL could incur more noticeable training costs.

6. Related Work

(Lu et al., 2024) propose a resettable scan operator specifically for the S5 model. (Blleloch, 1990) provide a resettable scan for quicksort, but provide no proof nor a general form. (Gu & Dao, 2023) unify a number of linear recurrent models as LTI systems, however, they do not provide a reset mechanism or generalize to non-linear recurrent updates.

There is prior work on special types of experience replay for recurrent models. (Hausknecht & Stone, 2015; Kap-turovski et al., 2019) find that warming up segment-based RNNs by replaying older segments can improve the return. However, implementing the warmup is difficult, and it is not clear that warming up the RNN is better than simply increasing the segment size by the warmup length.

7. Conclusion

We introduced memory monoids as a unifying framework for efficient sequence modeling. We found that memory monoids can represent a large number of efficient recurrent models, as well as the discounted return and the advantage. Using our resettable transformation, we extended our approach to encompass batching across variable length sequences. Given the efficiency of memory monoids over long sequences, we questioned whether the standard split-and-pad approach to POMDPs was still necessary. We found that said approach causes issues, with shorter segment lengths hampering sample efficiency and ultimately converging to lower returns. We proposed a simple change to batching methodology, that when combined with memory monoids, improves sample efficiency at a negligible cost.

Acknowledgements

We gratefully acknowledge the support of Toshiba Europe Ltd. This work was also supported in part by ARL DCIST CRA W911NF-17-2-0181 and European Research Council (ERC) Project 949940 (gAIa).

References

- Anonymous. Retentive Network: A Successor to Transformer for Large Language Models. In *Submitted to The Twelfth International Conference on Learning Representations*, 2023. URL <https://openreview.net/forum?id=UU9Icwbbhin>.
- Ba, J. L., Kiros, J. R., and Hinton, G. E. Layer normalization. *arXiv preprint arXiv:1607.06450*, 2016.
- Bauer, J., Baumli, K., Behbahani, F., Bhoopchand, A., Bradley-Schmieg, N., Chang, M., Clay, N., Collister, A., Dasagi, V., Gonzalez, L., Gregor, K., Hughes, E., Kashem, S., Loks-Thompson, M., Openshaw, H., Parker-Holder, J., Pathak, S., Perez-Nieves, N., Rakicevic, N., Rocktäschel, T., Schroecker, Y., Singh, S., Sygnowski, J., Tuyls, K., York, S., Zacherl, A., and Zhang, L. M. Human-timescale adaptation in an open-ended task space. In Krause, A., Brunskill, E., Cho, K., Engelhardt, B., Sabato, S., and Scarlett, J. (eds.), *Proceedings of the 40th International Conference on Machine Learning*, volume 202 of *Proceedings of Machine Learning Research*, pp. 1887–1935. PMLR, 23–29 Jul 2023. URL <https://proceedings.mlr.press/v202/bauer23a.html>.
- Blelloch, G. E. Prefix Sums and Their Applications. Technical report, School of Computer Science, Carnegie Mellon University, November 1990.
- Bourbaki, N. *Éléments de mathématique. Integration, Livre 1, Livre 5*, 1965. Publisher: Hermann Paris.
- Bradbury, J., Frostig, R., Hawkins, P., Johnson, M. J., Leary, C., Maclaurin, D., Necula, G., Paszke, A., VanderPlas, J., Wanderman-Milne, S., and Zhang, Q. JAX: composable transformations of Python+NumPy programs, 2018. URL <http://github.com/google/jax>.
- Dhulipala, L., Blelloch, G. E., and Shun, J. Theoretically Efficient Parallel Graph Algorithms Can Be Fast and Scalable. *ACM Trans. Parallel Comput.*, 8(1), April 2021. ISSN 2329-4949. doi: 10.1145/3434393. URL <https://doi.org/10.1145/3434393>. Place: New York, NY, USA Publisher: Association for Computing Machinery.
- Gu, A. and Dao, T. Mamba: Linear-time sequence modeling with selective state spaces. *arXiv preprint arXiv:2312.00752*, 2023.
- Gu, A., Johnson, I., Goel, K., Saab, K., Dao, T., Rudra, A., and Ré, C. Combining Recurrent, Convolutional, and Continuous-time Models with Linear State Space Layers. In *Advances in Neural Information Processing Systems*, volume 34, pp. 572–585. Curran Associates, Inc., 2021. URL <https://proceedings.neurips.cc/paper/2021/hash/05546b0e38ab9175cd905eebcc6ebb76-Abstract.html>.
- Hafner, D., Pasukonis, J., Ba, J., and Lillicrap, T. Mastering Diverse Domains through World Models. *arXiv preprint arXiv:2301.04104*, 2023.
- Hausknecht, M. and Stone, P. Deep Recurrent Q-Learning for Partially Observable MDPs. In *2015 AAAI Fall Symposium Series*, September 2015. URL <https://www.aaai.org/ocs/index.php/FSS/FSS15/paper/view/11673>.
- Huang, S., Dossa, R. F. J., Ye, C., and Braga, J. CleanRL: High-quality Single-file Implementations of Deep Reinforcement Learning Algorithms. 2021. eprint: 2111.08819.
- Ioffe, S. and Szegedy, C. Batch normalization: Accelerating deep network training by reducing internal covariate shift. In *International conference on machine learning*, pp. 448–456. pmlr, 2015.
- Kapturowski, S., Ostrovski, G., Quan, J., Munos, R., and Dabney, W. RECURRENT EXPERIENCE REPLAY IN DISTRIBUTED REINFORCEMENT LEARNING. pp. 19, 2019.
- Katharopoulos, A., Vyas, A., Pappas, N., and Fleuret, F. Transformers are RNNs: fast autoregressive transformers with linear attention. In *Proceedings of the 37th International Conference on Machine Learning, ICML’20*, pp. 5156–5165. JMLR.org, July 2020.
- Liang, E., Liaw, R., Nishihara, R., Moritz, P., Fox, R., Goldberg, K., Gonzalez, J., Jordan, M., and Stoica, I. RLlib: Abstractions for distributed reinforcement learning. In *International Conference on Machine Learning*, pp. 3053–3062. PMLR, 2018.
- Lu, C., Schroecker, Y., Gu, A., Parisotto, E., Foerster, J., Singh, S., and Behbahani, F. Structured state space models for in-context reinforcement learning. *Advances in Neural Information Processing Systems*, 36, 2024.
- Morad, S., Kortvelesy, R., Bettini, M., Liwicki, S., and Prorok, A. POPGym: Benchmarking Partially Observable Reinforcement Learning. In *The Eleventh International Conference on Learning Representations*, 2023a. URL <https://openreview.net/forum?id=chDrutUTs0K>.

- Morad, S., Kortvelesy, R., Liwicki, S., and Prorok, A. Reinforcement Learning with Fast and Forgetful Memory. In *Thirty-seventh Conference on Neural Information Processing Systems*, 2023b. URL <https://openreview.net/forum?id=KTfAtro6vP>.
- Orvieto, A., Smith, S. L., Gu, A., Fernando, A., Gulcehre, C., Pascanu, R., and De, S. Resurrecting Recurrent Neural Networks for Long Sequences. In *Proceedings of the 40th International Conference on Machine Learning*, ICML'23. JMLR.org, 2023. Place: Honolulu, Hawaii, USA.
- Peng, B., Alcaide, E., Anthony, Q., Albalak, A., Arcadinho, S., Biderman, S., Cao, H., Cheng, X., Chung, M., Grella, M., GV, K. K., He, X., Hou, H., Lin, J., Kazienko, P., Kocon, J., Kong, J., Koptyra, B., Lau, H., Mantri, K. S. I., Mom, F., Saito, A., Song, G., Tang, X., Wang, B., Wind, J. S., Wozniak, S., Zhang, R., Zhang, Z., Zhao, Q., Zhou, P., Zhou, Q., Zhu, J., and Zhu, R.-J. RWKV: Reinventing RNNs for the Transformer Era, December 2023. URL <http://arxiv.org/abs/2305.13048>. arXiv:2305.13048 [cs].
- Raffin, A., Hill, A., Gleave, A., Kanervisto, A., Ernestus, M., and Dormann, N. Stable-Baselines3: Reliable Reinforcement Learning Implementations. *Journal of Machine Learning Research*, 22(268):1–8, 2021. URL <http://jmlr.org/papers/v22/20-1364.html>.
- Schaul, T., Quan, J., Antonoglou, I., and Silver, D. Prioritized experience replay. *arXiv preprint arXiv:1511.05952*, 2015.
- Schlag, I., Irie, K., and Schmidhuber, J. Linear Transformers Are Secretly Fast Weight Programmers. In *Proceedings of the 38th International Conference on Machine Learning*, pp. 9355–9366. PMLR, July 2021. URL <https://proceedings.mlr.press/v139/schlag21a.html>. ISSN: 2640-3498.
- Schulman, J., Moritz, P., Levine, S., Jordan, M., and Abbeel, P. High-Dimensional Continuous Control Using Generalized Advantage Estimation. In *Proceedings of the International Conference on Learning Representations (ICLR)*, 2016.
- Serrano-Muñoz, A., Chrysostomou, D., Bøgh, S., and Arana-Arexolaleiba, N. skrl: Modular and Flexible Library for Reinforcement Learning. *Journal of Machine Learning Research*, 24(254):1–9, 2023. URL <http://jmlr.org/papers/v24/23-0112.html>.
- Van Hasselt, H., Guez, A., and Silver, D. Deep reinforcement learning with double q-learning. In *Proceedings of the AAAI conference on artificial intelligence*, volume 30, 2016. Issue: 1.
- Wang, Z., Schaul, T., Hessel, M., Hasselt, H., Lanctot, M., and Freitas, N. Dueling network architectures for deep reinforcement learning. In *International conference on machine learning*, pp. 1995–2003. PMLR, 2016.
- Xu, B., Wang, N., Chen, T., and Li, M. Empirical evaluation of rectified activations in convolutional network. *arXiv preprint arXiv:1505.00853*, 2015.

A. Return Comparison Between TBB and SBB

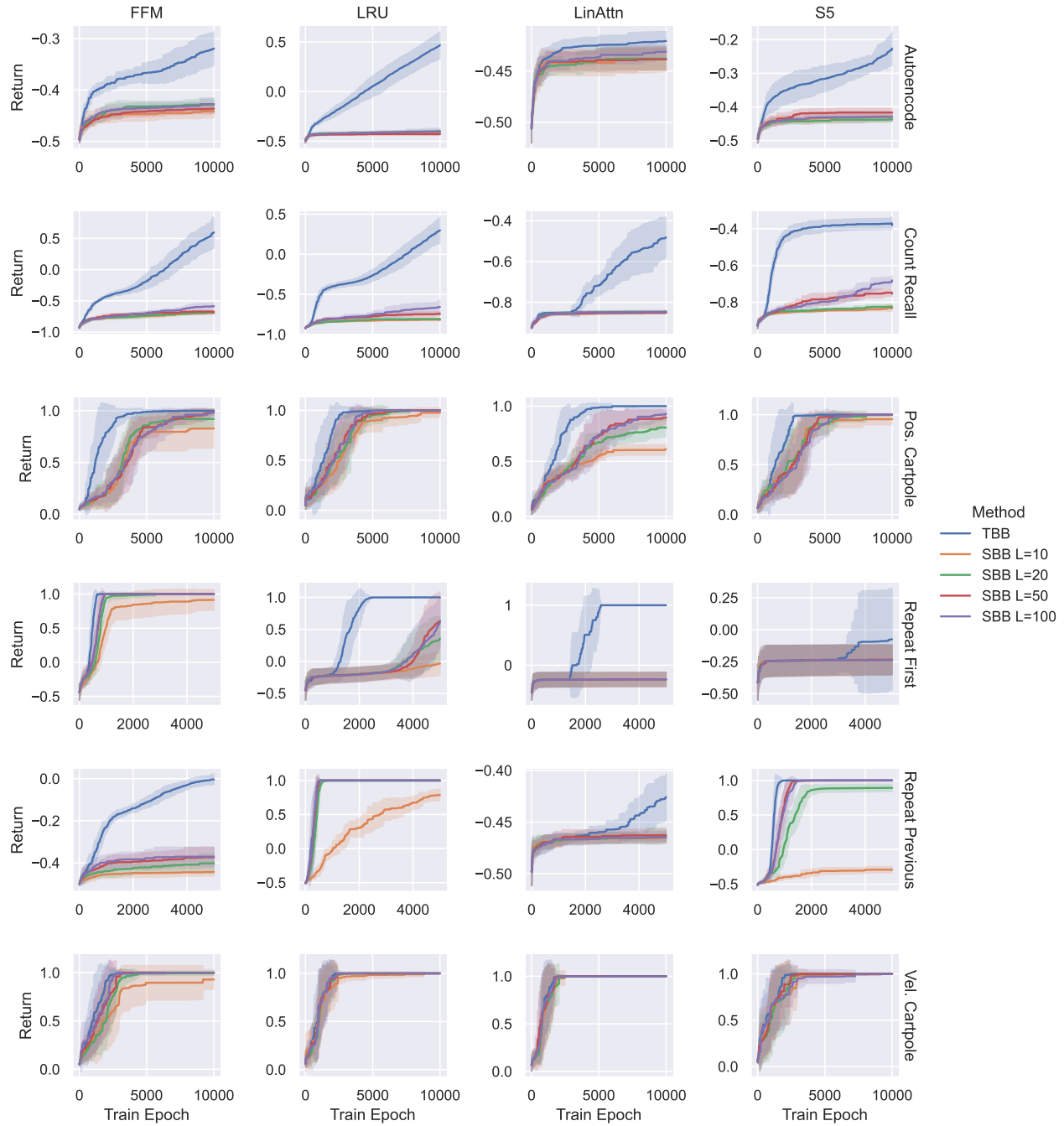


Figure 6. We run four memory monoids on six different POPGym environments over ten seeds and report the mean and 95% bootstrapped confidence interval. The POPGym environments have a minimum episodic return of -1.0 and a maximum of 1.0. In virtually all experiments, Tape-Based Batching provides improved sample efficiency over all tested segments length using Segment-Based Batching. The Count Recall and Autoencoder environments have temporal dependencies that span the entire sequence, demonstrating the importance of TBB for long range dependencies. On the other hand, Positional Cartpole has a temporal dependency of two timesteps, and so policies trained via SBB can still do reasonably well. Like Count Recall, Repeat First has long term temporal dependencies, however, SBB-trained methods do better than in Count Recall because Repeat First requires storing and recalling only a single observation.

B. Observation Sensitivity Analysis

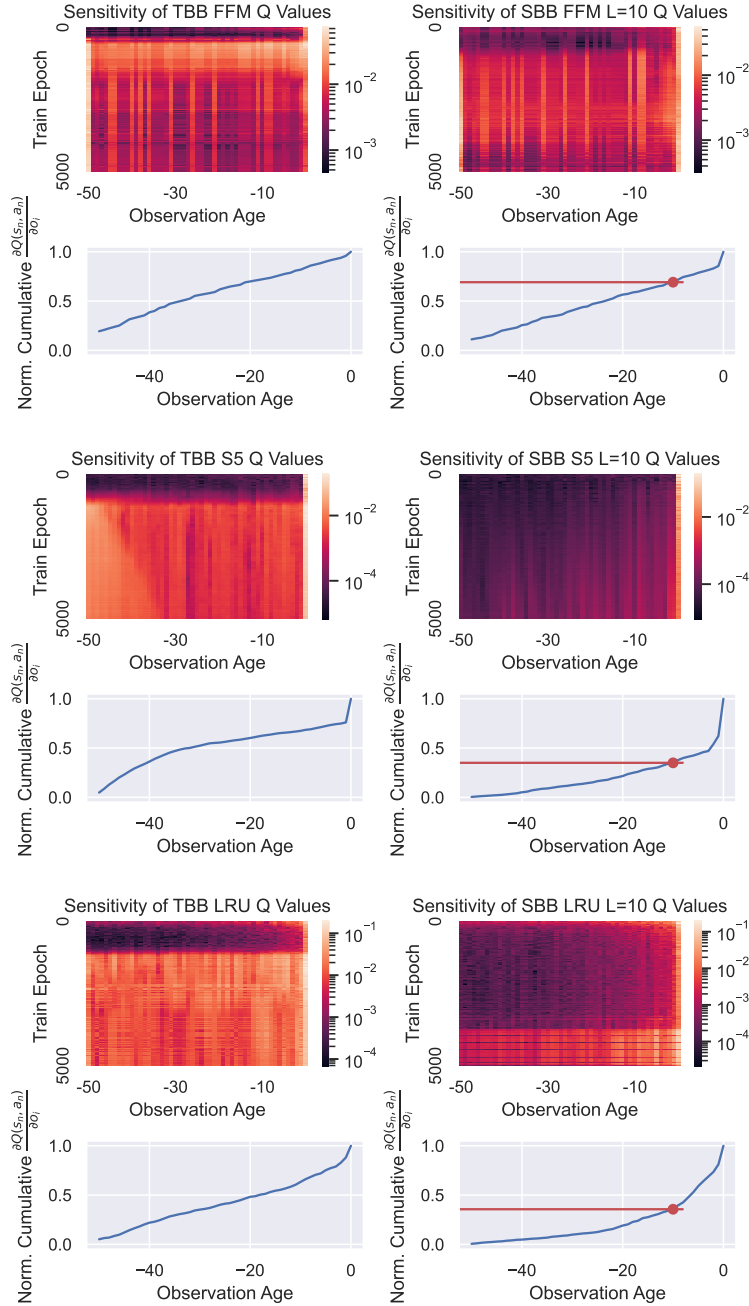


Figure 7. We follow a similar approach to Figure 3 for the Repeat First environment from the POPGym benchmark. At each timestep, the agent receives reward for outputting the initial observation. Unlike Repeat Previous, we expect that the initial observation should have a large contribution to the Q value. We see that for policies trained with TBB, the initial timestep contributes more to Q value than with SBB. In all cases, the Q value is still highly dependent on inputs that are not important.

C. Segment-Based Batching

After collecting episodes E during a rollout, we split E into fragments F such that each F has a maximum length of L . Fragments are zero padded from the right until they are precisely length L , turning them into segments σ and padding masks m . The segments are stacked into a dataset \mathcal{D} , enabling easy batching, storage, and training (Figure 1). We define this approach more accurately in the following paragraphs.

We define a segment σ as a length L sequence of transitions. During collection, episodes E longer than L transitions are *split* into fragments F . Fragments are then *zero-padded* to be length L , resulting in fixed-size segments σ and associated masks m . The resulting segments and masks are stacked into a dataset \mathcal{D} , enabling easy batching, storage, and training (Figure 1).

The split function splits a single episode E into one or more fragments F , each of size L except for the final fragment.

$$\begin{array}{cccc} F_0 & T_0, & T_1, & \dots & T_{L-1} \\ F_1 & T_L, & T_{L+1}, & \dots & T_{2(L-1)} \\ \vdots & \vdots & & & \\ F_k & T_{kL}, & \dots & & T_n \end{array} = \quad (31)$$

The pad function zero pads a fragment F into a fixed size segment σ and associated mask m denoting the padding elements

$$\sigma, m = \text{pad}(F, L) \quad (32)$$

$$= \text{concat}(F, 0^{L-\text{card}(F)}), \text{concat}(1^{\text{card}(F)}, 0^{L-\text{card}(F)}) \quad (33)$$

Using our split and pad operators, we split and pad each incoming episode, producing one or more segments and associated masks for each episode

$$\begin{bmatrix} \sigma_0, m_0 \\ \vdots \\ \sigma_k, m_k \end{bmatrix} = \text{pad}(F_i, L), \quad \forall F_i \in \text{split}(E, L). \quad (34)$$

We represent our training dataset \mathcal{D} as the concatenation of segments and masks

$$\mathcal{D} = \text{concat} \left(\begin{array}{c} \begin{bmatrix} \sigma_0, m_0 \\ \vdots \\ \sigma_k, m_k \end{bmatrix} \\ \begin{bmatrix} \sigma_{k+1}, m_{k+1} \\ \vdots \\ \sigma_j, m_j \end{bmatrix} \\ \vdots \end{array} \right) = \begin{bmatrix} \sigma_0, m_0 \\ \vdots \\ \sigma_k, m_k \\ \sigma_{k+1}, m_{k+1} \\ \vdots \\ \sigma_j, m_j \\ \vdots \end{bmatrix} \quad (35)$$

During training, we randomly sample rows from \mathcal{D} for minibatching (on-policy) or experience replay (off-policy).

D. Resettable Monoid Transformation Proof

Proof of Theorem 3.4. First, let us compute all possible pairs of inputs, as we will use them to simplify the rest of the proof.

$$(A, 0) \circ (A', 0) = (A \cdot (1 - 0) + H_I \cdot 0 \bullet A', 0 \vee 0) = (A \bullet A', 0) \quad (36)$$

$$(A, 1) \circ (A', 0) = (A \cdot (1 - 0) + H_I \cdot 0 \bullet A', 1 \vee 0) = (A \bullet A', 1) \quad (37)$$

$$(A, 0) \circ (A', 1) = (A \cdot (1 - 1) + H_I \cdot 1 \bullet A', 0 \vee 1) = (H_I \bullet A', 1) \quad (38)$$

$$(39)$$

Now, we must demonstrate that associativity holds $((A, b) \bullet (A', b')) \bullet (A'', b'') = (A, b) \bullet ((A', b') \bullet (A'', b''))$ for all possibilities of A, A', A'' and b, b', b'' . That is, we must ensure that the episode boundaries are correctly handled for all possibilities – that information does not leak across episode boundaries and that prior information otherwise propagates forward in time.

$$(A \bullet A', 0) \circ (A'', 0) = ((A \bullet A') \cdot (1 - 0) + H_I \cdot 0 \bullet A'', 0 \vee 0) = (A \bullet A' \bullet A'', 0) \quad (40)$$

$$(A \bullet A', 1) \circ (A'', 0) = ((A \bullet A') \cdot (1 - 0) + H_I \cdot 0 \bullet A'', 1 \vee 0) = (A \bullet A' \bullet A'', 1) \quad (41)$$

$$(H_I \bullet A', 1) \circ (A'', 0) = ((H_I \bullet A') \cdot (1 - 0) + H_I \cdot 0 \bullet A'', 1 \vee 0) = (H_I \bullet A' \bullet A'', 1). \quad (42)$$

And for $b'' = 1$, we have

$$(A \bullet A', 0) \circ (A'', 1) = ((A \bullet A') \cdot (1 - 1) + H_I \cdot 1 \bullet A'', 0 \vee 1) = (A \bullet A' \bullet A'', 1) \quad (43)$$

$$(A \bullet A', 1) \circ (A'', 1) = ((A \bullet A') \cdot (1 - 1) + H_I \cdot 1 \bullet A'', 1 \vee 1) = (H_I \bullet A'', 1) \quad (44)$$

$$(H_I \bullet A', 1) \circ (A'', 1) = ((H_I \bullet A') \cdot (1 - 1) + H_I \cdot 1 \bullet A'', 1 \vee 1) = (H_I \bullet A'', 1). \quad (45)$$

We see that resets correctly remove the impact of any terms that occur before $b' = 1$, while correctly propagating state when $b' = 0$. \square

E. Proof of the Return as a Memory Monoid

Proof of Theorem 3.3. We prove the correctness of our discounted return memory monoid by showing the expansion is equivalent to the discounted return.

$$(1, 0) \bullet (\gamma, r_0) = (\gamma, r + 0) = (\gamma, r) \quad (46)$$

$$(1, 0) \bullet (\gamma, r_0) \bullet (\gamma, r_1) = (1 \cdot \gamma \cdot \gamma, 0 + 1 \cdot r_0 + \gamma r_1) = (\gamma^2, r_0 + \gamma r_1) \quad (47)$$

$$(1, 0) \bullet (\gamma, r_0) \bullet \dots \bullet (\gamma, r_n) = (1 \cdot \gamma \cdot \gamma \cdots \gamma, 1 \cdot r_0 + \gamma r_1 + \dots + \gamma^n r_n) \quad (48)$$

$$= \lim_{n \rightarrow \infty} \left(\gamma^n, \sum_{i=0}^n \gamma^i r_i \right) \quad (49)$$

□

F. The Generalized Advantage Estimate as a Memory Monoid

Let us define Generalized Advantage Estimation (GAE) in memory-monoid form:

Theorem F.1. *The GAE target given by*

$$A_t = \sum_{l=0}^{\infty} (\lambda\gamma)^l \delta_{t+l}; \quad \delta_t = r_t + \gamma V(s_{t+1}) - V(s_t) \quad (50)$$

is equivalent to computing M over $\delta_t, \delta_{t+1}, \dots$ for the given memory monoid:

$$H = \{(a, g) \mid a \in [0, 1], g \in \mathbb{R}\} \quad (51)$$

$$H_I = (1, 0) \quad (52)$$

$$(a, g) \bullet (a', g') = (aa', ag' + g) \quad (53)$$

$$f(o, b) = (\gamma\lambda, o) \quad (54)$$

$$g((a, g), (o, b)) = g. \quad (55)$$

Proof. We prove the correctness of our GAE memory monoid by showing the expansion is equivalent to the discounted return. This proof is very similar to the proof of the discounted return.

$$(1, 0) \bullet (\gamma\lambda, \delta_t) = (\gamma\lambda, \delta_t + 0) = (\gamma\lambda, \delta_t) \quad (56)$$

$$(1, 0) \bullet (\gamma\lambda, \delta_t) \bullet (\gamma\lambda, \delta_{t+1}) = (1 \cdot \gamma\lambda \cdot \gamma\lambda, 0 + 1 \cdot \delta + \gamma\lambda\delta_{t+1}) = ((\gamma\lambda)^2, \delta + \gamma\lambda\delta_{t+1}) \quad (57)$$

$$(1, 0) \bullet (\gamma\lambda, \delta_t) \bullet \dots \bullet (\gamma\lambda, \delta_{t+n}) = (1 \cdot \gamma\lambda \cdot \gamma\lambda \cdot \dots \cdot \gamma\lambda, 1 \cdot \delta + \gamma\lambda\delta_{t+1} + \dots + (\gamma\lambda)^n \delta_{t+n}) \quad (58)$$

$$= \lim_{n \rightarrow \infty} \left((\gamma\lambda)^n, \sum_{l=0}^n (\gamma\lambda)^l \delta_{t+l} \right) \quad (59)$$

□

G. Rewriting Sequence Models as Memory Monoids

In this section, we reformulate existing models used in our experiments as memory monoids. This reformulation is necessary to use inline resets for these models. Prior work (Lu et al., 2024) defines an associate scan operator for the S5 variant of State Space Models. Little work is required to rewrite this in memory monoid form:

$$H = \{(A, a) \mid A \in \mathbb{C}^{m \times m}, a \in \mathbb{R}^{m \times 1}\} \quad (60)$$

$$H_I = (I_m, 0) \quad (61)$$

$$(A, a) \bullet (A', a') = (A'A, A'a + a') \quad (62)$$

$$f(o, b) = (W_A, W_a o) \quad (63)$$

$$g((A, a), (o, b)) = (W_1 \text{GeLU}(W_c a) + b_1) \odot \text{sigmoid}(W_2 \text{GeLU}(W_c a) + b_2) \quad (64)$$

where W_A, W_b, W_c are learnable weights, b_1, b_2 are learnable biases, and I_m is the square identity matrix of size m . The Linear Recurrent Unit (Orvieto et al., 2023) could be roughly described as a theoretical simplification of S5, bringing it closer to classical RNNs. Writing it out as a memory monoid, we see that it is nearly identical to S5, however the weight initialization is different

$$H = \{(A, a) \mid A \in \mathbb{C}^{m \times m}, a \in \mathbb{C}^{m \times 1}\} \quad (65)$$

$$H_I = (I_m, 0) \quad (66)$$

$$(A, a) \bullet (A', a') = (A'A, A'a + a') \quad (67)$$

$$f(o, b) = (W_A, W_a o) \quad (68)$$

$$g((A, a), (o, b)) = \text{MLP}(a) \quad (69)$$

Finally, we can rewrite Fast and Forgetful Memory (FFM) as a memory monoid, with the parallel scans simplifying its implementation and fixing numerical instabilities caused by large positive exponentials over long sequences, as discussed in (Morad et al., 2023b).

$$H = \{(A, t) \mid A \in \mathbb{C}^{m \times c}, t \in \mathbb{Z}\} \quad (70)$$

$$H_I = (0, 0) \quad (71)$$

$$(A, t) \bullet (A', t') = (A \odot \exp(t'(-|\alpha| \oplus i\omega)) + A', t + t') \quad (72)$$

$$f(o, b) = \left(\begin{array}{c} [(W_1 o + b_1) \odot \sigma(W_2 o + b_2)]^\top \\ \vdots \\ [(W_1 o + b_1) \odot \sigma(W_2 o + b_2)] \end{array} , 1 \right) \quad (73)$$

$$g((A, t), (o, b)) = \text{MLP}(\text{LN}(W_3 [\Re(A) \parallel \Im(A)] + b_3)) \odot \sigma(W_4 o + b_4)(1 - \sigma(W_4 o + b_4)) \odot o \quad (74)$$

where W, b are learnable weights and biases, \Re, \Im extract the real and imaginary part of a complex number, \odot is the elementwise product, \oplus is an outer sum, and $\alpha \in \mathcal{R}^n, \omega \in \mathcal{R}^m$ are learnable parameters. We note that unlike the other examples, FFM is a time-varying recurrence because the recurrent updates depends on t .

H. Non-Recurrent Q Learning

Algorithm 5 Non-recurrent Q learning update

Input: params θ , target params ϕ , Q function Q , train batch \mathcal{B} , discount γ

$$\hat{y}_j = r_j + \max_{a \in A} \gamma Q_\phi(s'_j, a), \quad \forall \mathcal{B}[j]$$

$$\theta \leftarrow \min_{\theta} \|Q_\phi(s_j, a_j) - \hat{y}_j\|, \quad \forall \mathcal{B}[j]$$

$$\phi \leftarrow \phi\beta + (1 - \beta)\theta$$

{Q Target}

{Q update}

{Target update}

I. Experiment Setup

We used the same model hyperparameters across all experiments. Training hyperparameters, such as number of epochs, varied across tasks.

I.1. Model Setup

We construct our model using blocks. A block contains a linear layer with nonparametric layer normalization and leaky ReLU activation. Observations feed into a block, followed by a memory model, followed by two more blocks. The hidden size of all blocks is 256 dimensions. For the S5 and LRU models, stacked two S5 and LRU layers, resulting in a sum of 512 dimensions of recurrent state (256 per layer). The Linear Transformer and Fast and Forgetful Memory models use just a single layer with 256 dimensions of recurrent state. We use the ADAM optimizer without weight decay.

I.2. Task Setup

For each task, we selected a replay buffer large enough such that no old observations ever needed to be discarded. Epochs Rand, Train describes the number of episodes we collect randomly, and then the number of training epochs. Polyak τ determines the target network update rate. Batch Size measures the batch size in transitions for each model update. LR is the learning rate with a linear warmup over a specified number of model updates. The train ratio describes the number of episodes collected at each epoch, compared to the number of model updates per epoch. ∇ Clip corresponds to gradient clipping, where the gradient magnitude is rescaled to at most ∇ Clip. γ is the decay term used in MDPs.

Task	Epochs Rand, Train	Polyak τ	Batch Size	LR, Warmup	Train Ratio	∇ Clip	γ
RepeatFirst	5,000 (5,000)	0.995	1,000	0.0001 (200)	1:1	0.01	0.99
RepeatPrevious	5,000 (5,000)	0.995	1,000	0.0001 (200)	1:1	0.01	0.5
CountRecall	10,000 (10,000)	0.995	1,000	0.0001 (200)	1:1	0.01	0.99
PosOnlyCartPole	10,000 (10,000)	0.995	1,000	0.0001 (200)	1:1	0.01	0.99
VelOnlyCartPole	10,000 (10,000)	0.995	1,000	0.0001 (200)	1:1	0.01	0.99
AutoEncode	10,000 (10,000)	0.995	1,000	0.0001 (200)	1:4	0.01	0.99

J. Glossary of Symbols

Symbol	Meaning
S	State space
A	Action space
R	Reward function
\mathcal{T}	State transition function
γ	Discount factor
s	Markov state
a	action
r	reward
s'	next state
d	Done flag
b	Begin flag
\mathcal{O}	Observation function
O	Observation space
o	Observation
T	Transition (o, a, r, o', d, b)
\bar{T}	Partial transition (o, b)
ρ	Rollout
E	Episode of transitions
L	Segment length
\mathcal{D}	Dataset
\mathcal{B}	Train batch
B	Batch size
σ	Segment
m	Boolean mask for segment
\mathcal{L}	Loss function
θ	Model parameters
H	Set of recurrent states
H_I	An identity element in H
\bullet	A monoid binary operator
f	A mapping from a partial transition to H
g	A mapping from H and O to the Markov state S
M	Memory model that summarizes a sequence of transitions
n	Length of a sequence
G	Both the discounted return and the set of resettable monoid recurrent states
G_I	The identity element in G
\circ	A resettable monoid binary operator
\vee	Logical or
pad	An operation that right zero pads a vector to a specified length
split	Splits a long episode into subsequences of length $\leq L$
concat	A vector/matrix concatenation operator
card	The cardinality of the argument

Table 2. A glossary of symbols